HHS Public Access

Author manuscript

Oncogene. Author manuscript; available in PMC 2020 May 19.

Published in final edited form as:

Oncogene. 2020 February ; 39(9): 1831–1845. doi:10.1038/s41388-019-1102-1.

Chemotherapy impacts on the cellular response to CDK4/6 inhibition: distinct mechanisms of interaction and efficacy in models of pancreatic cancer

Vishnu Kumarasamy[1,3], **Amanda Ruiz**[4], **Ram Nambiar**[1,3], **Agnieszka K. Witkiewicz**[1,2,*], **Erik S. Knudsen**[1,3,*]

[1]Center for Personalized Medicine, Roswell Park Cancer Institute, Buffalo NY

[2]Department of Pathology, Roswell Park Cancer Institute, Buffalo NY

[3]Department of Molecular and Cellular Biology, Roswell Park Cancer Institute, Buffalo NY

[4]Arizona Cancer Center, University of Arizona, Tucson AZ

Abstract

Pancreatic ductal adenocarcinoma (PDAC) is a therapy recalcitrant disease characterized by the aberrations in multiple genes that drive pathogenesis and limit therapeutic response. While CDK4/6 represents a downstream target of both KRAS mutation and loss of the CDKN2A tumor suppressor in PDAC, clinical and preclinical studies indicate that pharmacological CDK4/6 inhibitors are only modestly effective. Since chemotherapy represents the established backbone of PDAC treatment we evaluated the interaction of CDK4/6 inhibitors with gemcitabine and taxanes that are employed in the treatment of PDAC. Herein, we demonstrate that the difference in mechanisms of actions of chemotherapeutic agents elicit distinct effects on the cellular response to CDK4/6 inhibition. Gemcitabine largely ablates the function of CDK4/6 inhibition in S-phase arrested cells when administered contemporaneously; although, when cells recover from S-phase block they exhibit sensitivity to CDK4/6 inhibition. In contrast, pharmacological inhibition of CDK4/6 yields a cooperative cytostatic effect in combination with docetaxel and prevents adaptation and cell cycle re-entry, which is a common basis for resistance to such agents. Importantly, using organoid and PDX models we could confirm the cooperative effects between chemotherapy and CDK4/6 inhibition. These data indicate that the combination of cytotoxic and cytostatic agents could represent an important modality in those tumor types that are relatively resistant to CDK4/6 inhibitors.

*__Correspondence:__ Agnieszka K. Witkiewicz, Center for Personalized Medicine, Roswell Park Cancer Center, Agnieszka.Witkiewicz@Roswellpark.org, Erik S. Knudsen, Department of Molecular and Cellular Biology, Roswell Park Cancer Institute, Buffalo NY, Erik.Knudsen@roswellpark.org.

Role in Study:

Study concept and design: VK, ESK and AKW

Acquisition of data: VK, AR and RN

Analysis and interpretation of data: VK, ESK and AKW

Study supervision: ESK and AKW.

Introduction

Pancreatic ductal adenocarcinoma (PDAC) is the most common and aggressive malignancy of the pancreas with a 5-year survival rate of 5–10% (1–3). The reason for high mortality rate is that most of the pancreatic cancer patients harbor metastatic disease at the time diagnosis, which renders the standard therapeutic options, such as surgical resection and radiation therapy, futile (4). Systemic therapy for advanced pancreatic cancer involves the use chemotherapy drugs such as gemcitabine and taxanes (5, 6). To date, using molecular-targeted agents (e.g. erlotinib) has had minimal positive impact on patient survival, thereby illustrating the need for new potent therapeutic options (7). Since PDAC is a molecularly-diverse disease exhibiting a range of genetic alterations, it provides potential opportunities to develop a rationally targeted therapy (1, 8–10).

Multiple genetic aberrations occurring in PDAC converge in the deregulation of the cyclin dependent kinases CDK4 and CDK6 that drive G1-S phase transition of the cell cycle through the inactivation of RB pathway (11–13). Mutant KRAS signaling coalesces in the induction of D-type cyclins that enhances the kinase activities of CDK4 and CDK6 (14, 15). Moreover, the loss of a tumor suppressor gene, *CDKN2A*, which encodes an endogenous CDK4/6 inhibitor, further deregulates the kinase activity (8, 11, 16). While targeting the function of CDK4/6 to re-establish cell cycle inhibition in PDACs would appear to represent a successful therapeutic strategy, PDACs develop adaptive resistant mechanisms to CDK4/6 inhibitors (17, 18). Notably, in a previous study, PDAC models possessed cell cycle plasticity that enabled them to escape CDK4/6 inhibition, which could be prevented by combining with agents that target KRAS effector pathways (17, 19). This feature of PDAC drives the focus on developing a therapeutic strategy by combining CDK4/6 inhibitors with other agents that are clinically active.

Here we investigated whether combining CDK4/6 inhibitors with the chemotherapy agents, gemcitabine and taxane could represent a potential opportunity for enhancing disease control and durability of response in PDAC models. Although there are preclinical evidences in different cancer models to support that CDK4/6 inhibitors could cooperate with chemotherapy to elicit improved disease control, the mechanism of interaction between these agents remains unclear (20–22). For instance, CDK4/6 inhibitors have the potential to antagonize acute cytotoxic response to different forms of chemotherapy in certain types of breast cancer and normal hematopoietic stem cells (23–25). Conversely, in specific setting there seems to be cooperative activities between CDK4/6 inhibition and chemotherapy that appear clinically active (26, 27). Since there are multiple ongoing clinical trials involving the combination of chemotherapy with CDK4/6 inhibitors in patients, understanding both acute and long-term responses to such combination treatment regimen is of clear importance.

Results

PDAC models bypass pharmacological inhibition of CDK4/6 activity

In this study, we investigated the cellular response of CDK4/6 inhibition in different patient-derived primary PDAC cells (1222, 3226, 226 and 7310) (19). These models exhibit genetic features representative of the primary tumor from which they were isolated and harbor

KRAS mutations, SMAD4, and TP53 mutations that are present in PDAC tumors (28) (Fig. S1). Cell cycle analysis indicates that the PDAC models, 1222, 3226 and 226, possessed only a partial cytostatic response as observed by a modest increase in the population of cells at G1-phase (Fig. 1A). To validate the on-target effect of palbociclib, we utilized an RB-negative PDAC model, 7310, which was completely unresponsive to palbociclib (Fig. 1A). To demonstrate the cytostatic effect of palbociclib at these doses, we employed ER^+ breast cancer MCF7 cell line as a control, which has been previously shown to be highly sensitive to CDK4/6 inhibition (29, 30). Consistent with previous studies, MCF7 cells displayed prominent G1-arrest, associated with a significant decrease in the population of cells at S-phase (Fig. 1B). Similar differential responses were observed when the PDAC and MCF7 cells were treated with ribociclib and abemaciclib (Fig S1). Even after 5-day treatment with CDK4/6 inhibitors, the PDAC models only possessed partial cytostatic effect at non-therapeutic doses (Fig. S1). Biochemical analysis revealed that PDAC cells exhibited partial inhibition of RB phosphorylation in the presence of palbociclib and maintained the expression of cyclin A, which is a downstream E2F-regulated target (Fig. 1C). However, in MCF7 cells, palbociclib resulted in complete dephosphorylation of RB and veritably complete loss of cyclin A expression (Fig. 1C). We performed RNA sequencing in PDAC models and MCF7 cells to determine the effect of palbociclib on RB/E2F-target genes. The downregulated genes in all the PDAC models were identified based on average fold-repression that is statistically significant. Gene ontology analysis indicates that these genes are associated with cell-cycle, DNA replication and DNA repair (Fig S1, Table S1). In MCF7 cells, palbociclib displayed repression of similar genes but the magnitude of repression was much stronger as compared to the PDAC models (Fig. 1D). The transcriptional repression of the RB/E2F target genes by palbociclib was also observed in multiple PDX models, indicating that CDK4/6 inhibition while not completely inhibiting cell cycle in PDAC models does impinge on processes that are related to chemotherapy response (Fig S1, Table S2).

It is emerging that the coupling of CDK4/6 inhibition with downstream suppression of CDK2 activity is critically important for therapeutic response. We found that treatment with palbociclib strongly inhibited the CDK2 activity in MCF7 cells, while in the PDAC cell line (1222) the kinase activity was only modestly inhibited (Fig. 1E). The partial inhibition of CDK2 kinase activity in PDAC by palbociclib is associated with increased complex of cyclin E1 with CDK2, which was not observed in MCF7 cells (Fig. 1E). CDK2 kinase activity was not modulated in the RB^{null} 7310 cell line in the presence of palbociclib, suggesting that the predominant cytostatic effect of RB-dependent action is driven through CDK2 kinase blockade (Fig. 1E). Taken together, it is evident that the PDAC cells are relatively resistant to CDK4/6 inhibition as monotherapy by escaping the negative cell-cycle regulation through the CDK2 kinase axis.

Effect of CDK4/6 inhibition on the response to gemcitabine in PDAC models

Prior studies have evaluated the impact of CDK4/6 inhibitors on response to gemcitabine and shown evidence for both antagonism and cooperation (22, 23). Therefore, we interrogated the interaction between gemcitabine and palbociclib in our models. Following the exposure to gemcitabine (500 nM), PDAC cells (1222 and 3226) exhibited an increase in

the population of cells at S-phase (Fig. 2A and Fig. S2). However, concurrent or 24 h pretreatment with palbociclib did not alter the cell-cycle distribution induced by gemcitabine treatment (Fig. 2A and Fig. S2), which presumably reflects the dominant action of gemcitabine in these models. To interrogate the impact of palbociclib on gemcitabine-induced DNA damage, γH2AX foci formation was determined in the PDAC cells (1222 and 3226) by immunofluorescence (31). PDAC cells treated with gemcitabine harbored a significant increase in the γH2AX foci, which was unaltered with palbociclib treatment (Fig. 2B and Fig S2). Biochemical analysis revealed that gemcitabine leads to depletion of cyclin D1 but results in the accumulation of cyclin A with corresponding increase in the phosphorylation of RB (Fig. 2C) (32, 33). Strikingly, these molecular events were not modulated by palbociclib indicating that the effect of CDK4/6 inhibition is largely obviated in the context of the dominant S-phase arrested induced by gemcitabine in PDAC cell lines (1222 and 3226) (Fig. 2C). Consistent with these features of response, rather than limiting kinase activity, palbociclib in combination with gemcitabine leads to enhanced CDK2 activity associated with cyclin A (Fig. 2D). Since, palbociclib had no effect relative to cell cycle in S-phase, it further failed to modulate the acute cytotoxicity and apoptotic signaling, induced by gemcitabine, as determined by cell-viability assays and PARP cleavage, respectively (Fig. 2E and Fig S2) (34). These data are discordant with the concept that CDK4/6 inhibition can antagonize response to chemotherapy. To determine if these features of combinatorial response was associated with limited cell cycle arrest, we depleted Cyclin E1 using gene-specific siRNA that showed dramatic cooperation with palbociclib to inhibit S-phase entry (Fig. 2F and Fig. S2). Under this condition the PDAC cell line (1222) was significantly protected from the gemcitabine-induced S-phase arrest (Fig. 2F). These data illustrate the importance of full vs. limited cell cycle inhibition on the interaction with chemotherapeutic agents.

The effect of CDK4/6 inhibition on the viability of PDAC cells following gemcitabine treatment was determined by colony out-growth assay. PDAC cells were treated with gemcitabine (100 nM) for 48 h and then allowed to recover in the absence and presence of palbociclib for the indicated time periods and stained with crystal violet to estimate the post-treatment out-growth. Following gemcitabine treatment, PDAC cells have the potential to retain their viability, which allows them to repopulate the culture (Fig 2G). This phenomenon was inhibited in the presence of palbociclib, suggesting that the ability of CDK4/6 inhibitor to downregulate the genes required for cell-cycle and DNA repair could prevent re-entry of cells to cell-cycle progression following the recovery from gemcitabine (19). Consistent with this notion, palbociclib enhanced the suppressive effect on the G1-phase cyclins, DNA replication as determined by BrdU incorporation and RB-regulated DNA repair genes FANCD2 and RAD51 following the removal of gemcitabine (Fig. 2H, 2I and Fig. S2) (35, 36). Overall these data indicate that the dosing schedule of CDK4/6 inhibitor is critical to therapeutic outcome when used in combination with drugs that are active in S-phase.

Cooperative effect of CDK4/6 inhibition with taxanes

Taxanes are used for the treatment of advanced pancreatic cancer patients, and as with gemcitabine there are conflicting results related to the intersection with CDK4/6 inhibitors

(6, 25). By flow cytometric analysis it is evident that docetaxel (taxane) resulted in the accumulation of cells at 4N state, accompanied by a pronounced population of cells with greater than 4N DNA content. (Fig. 3A, Fig S3) (37, 38). Interestingly, the inclusion of CDK4/6 inhibitors, palbociclib and ribociclib significantly suppressed the population of cells with greater than 4N DNA content, with surprisingly limited impact on the 2N population. To investigate whether the 4N cells correspond to mitotic arrest, immunoblot analysis were performed in 1222 and 226 cells to determine the levels of cyclin B1 and CDK1 (39). Docetaxel alone did not alter the expression of cyclin B1 and CDK1 and concurrent and 24-h pretreatment with palbociclib resulted in cooperative suppression of these proteins (Fig. 3B). Further examination of the nuclei of PDAC cells revealed that the phosphorylation of Ser10-Histone H3 occurred as an acute response to docetaxel, whereas, 48-hour exposure resulted only in aberrant nuclei without pHH3 foci (Fig. 3C). Overall, these data indicate that the 4N cells undergo re-replication following docetaxel treatment, which is inhibited by CDK4/6 inhibitors, leading to a tetraploid G1 arrest. To validate this phenomenon, PDAC cells were subjected to bi-variate flow cytometry (BrdU and propidium iodide). In the presence of docetaxel, the cells with 4N DNA content incorporated BrdU, which confirms the re-replication of these cells, whereas, the inclusion of CDK4/6 inhibitors cooperatively inhibited BrdU incorporation in both 2N and 4N cells (Fig. 3D, Fig S3). These data demonstrate that there is a cooperative interaction between taxanes and CDK4/6 inhibition in limiting DNA replication.

Mechanistic analysis of cooperative interaction

To interrogate the mechanisms of cooperation between CDK4/6 inhibition and taxanes, biochemical analysis was performed on proteins controlling the S-phase entry in the PDAC models (3226, 1222, 226 and 97). The treatment with CDK4/6 inhibition increases the protein levels of cyclin D1 and cyclin E1 in all the PDAC models, which is consistent with previous studies (Fig. 4A, Fig S4) (17, 19, 29). Strikingly, combination treatment with docetaxel prevented the accumulation of cyclin D1 and cyclin E1 that resulted in the cooperative downregulation of cyclin A and dephosphorylation of RB, which are the indicative markers of G1-arrest (Fig. 4A, Fig S4). These responses were also associated with the enhanced inhibition of cyclin A associated CDK2 kinase activity that governs DNA replication (Fig. 4B). These molecular events are consistent with the cell cycle analysis, confirming that the accumulation of 4N cells in the presence CDK4/6 inhibitors in combination with docetaxel is a result of cooperative response to limit DNA replication. To investigate that palbociclib inhibits the re-replication of 4N cells through its mechanistic target, we used the RB^{null} 7310 cells as control. In the presence of docetaxel, the 7310 cells with 4N DNA content underwent re-replication, which was not inhibited by palbociclib, confirming its dependency on RB (Fig. 4C). Immunoblot analysis further confirms that the cyclin B1, CDK1 and cyclin A protein expressions in 7310 cells were not modulated in the presence of palbociclib and docetaxel (Fig. 4D). To determine if cyclin E1 is the key determinant in the response to the combination treatment, we depleted the endogenous cyclin E1 expression using CCNE1 siRNA in 1222 and 226 PDAC models and the cells were exposed to docetaxel and palbociclib. CCNE1 knockdown inhibited the replication of 4N cells in the presence of docetaxel as determined by BrdU incorporation (Fig. 4E). Moreover, palbociclib in combination with docetaxel (Palbo/Doce) following CCNE1

knockdown inhibited the accumulation of 4N cells with a corresponding increase in 2N population and a pronounced inhibition of BrdU incorporation (Fig. 4E and Fig S4). Biochemical analysis revealed that cyclin E1 knockdown enhances the effect of palbo/doce on suppression of cyclin A, cyclin B1 and CDK1 proteins (Fig. 4F). Taken together, our data indicates that the docetaxel-mediated replication of 4N cells is driven by the CDK4/6 kinase that activates cyclin E1/CDK2 pathway and this mechanism could be potentially suppressed by CDK4/6 inhibitors in an RB dependent manner. Moreover, docetaxel cooperates with CDK4/6 inhibition by blocking the adaptive regulation of cyclin E1.

CDK4/6 inhibition yields cooperative effect with chemotherapy regimens

The influence of CDK4/6 inhibition on the cytotoxic effects of docetaxel in PDAC cells was by monitored by the poly ADP-ribose polymerase (PARP) cleavage. The basal levels of PARP cleavage remains unaltered in the presence of palbociclib, whereas exposure to docetaxel resulted in an enhanced PARP cleavage (Fig. 5A). However, concurrent treatment or 24 h pretreatment with palbociclib did not modulate the cleaved PARP protein across the evaluated cell models (Fig. 5A). Furthermore, the viability of the PDAC cells following 96 h exposure to docetaxel was also not modulated in the presence of palbociclib, suggesting that the acute cell-death mechanisms induced by taxanes remain unaltered irrespective of CDK4/6 inhibition (Fig. 5B, Fig S4). Since, docetaxel exerts its cytotoxic effect by targeting cells with 4N DNA content, we depleted CDK2 expression using gene specific siRNA, which prevented the progression of cells through S-phase in the presence of palbociclib. Under this condition, the PDAC cells were completely protected from the cellular and cytotoxic effects of docetaxel (Fig. 5C & Fig S4). To assess the long-term impact of CDK4/6 inhibitors on cell viability, colony outgrowth assays were performed. Palbociclib addition prevented clonal-outgrowth of PDAC cells (1222, 226 and 3226) that were released from docetaxel, presumably by preventing the re-entry of cells back into the cell cycle (Fig. 5D). Since gemcitabine in combination with taxanes is the standard of care for the PDAC treatment in the clinical setting, we evaluated the impact of CDK4/6 inhibitors on this therapeutic regimen. Following the release from the concurrent treatment of gemcitabine and docetaxel only fewer cells possessed the potential to retain their viability as compared to the single chemotherapeutic agent (Fig. 5E). Interestingly, both palbociclib and ribociclib resulted in little to no colony outgrowth specifically in RB proficient PDAC models, as the cellular outgrowth in the RB^{null} 7310 cell line was not inhibited by CDK4/6 inhibition (Fig. 5E).

Effect of CDK4/6 inhibition in combination with chemotherapy in PDAC organoids and PDX models

To determine the efficacy of multiple CDK4/6 inhibitors with single and combinatorial chemotherapy (gemcitabine and docetaxel) organoid cell cultures were deployed. In all the PDAC models evaluated, the combined chemotherapy treatment cooperatively inhibited the organoid growth as compared to the single agents (Fig. 6A). Interestingly, the addition of CDK4/6 inhibitors significantly enhanced the effect of gemcitabine and docetaxel on the viability of the organoids (Fig. 6A). To interrogate the *in vivo* efficacy of the CDK4/6 inhibitors in combination with gemcitabine and docetaxel treatment multiple different PDX models (1222, 3226 and 97) were employed. The treatment conditions were well tolerated as

no significant mouse weight loss was observed (Fig. S5). As shown in the Fig. 6B & C the triple combination treatment, involving palbociclib and ribociclib along with gemcitabine and docetaxel significantly suppressed the tumor growth in both 1222 and 3226 PDX models. Moreover, the CDK4/6 inhibitors potentiated the efficacy of gemcitabine and docetaxel treatment regimen through a profound increase in disease control across the PDX models, which was associated with the inhibition of tumor growth (Fig. 6D). In an additional PDX model (97), the triple combination group significantly delayed the tumor progression following the cessation of treatment (Fig. S5). These efficacy data are consistent with similar findings with independent PDX models. Overall, CDK4/6 inhibitors enhance the therapeutic efficacy of the chemotherapy drugs by inducing a durable control of tumor growth in patient-derived PDAC models.

Discussion

The pathogenesis of pancreatic ductal adenocarcinoma (PDAC) is driven by multiple genetic events (e.g. KRAS mutation and loss of CDKN2A) that yield deregulation of the CDK4/6-cyclin D pathway and results in aberrant cell-cycle progression (8, 11, 40, 41). However, the therapeutic efficacy of clinically approved CDK4/6 inhibitors as monotherapies in PDAC is largely undermined by compensatory cell cycle regulatory pathways (17, 18). As shown in our study, the degree of cell cycle inhibition by CDK4/6 inhibitors is considerably more modest in PDAC models as compared to the response in ER^+ breast cancer models. This condition of baseline resistance has also been observed in other RAS-driven tumors; therefore, significant efforts have focused on developing novel combination therapies (42, 43). Typically, such combinatorial approaches involve the use of different molecular targeted agents (e.g. MEK or MTOR inhibitors) along with CDK4/6 inhibitors to enforce durable response in different tumor types including PDAC models (17, 19). Although chemotherapeutic agents represent one of the most commonly used treatment options for metastatic cancer types, in certain contexts, combination with CDK4/6 inhibitors could potentially block the cells from cycling through chemotherapy-induced cytotoxicity (23, 44, 45). Such antagonistic modes of interaction are mainly observed in tumor models that are highly sensitive to CDK4/6 inhibitors (24, 25). Given that PDAC models possess limited response to CDK4/6 inhibitors that allows them to progress through cell-cycle, there could be room to either enhance their cytostatic effect in combination with chemotherapy or limit the recovery from the chemotherapy regimen.

In this study we investigated the efficacy of CDK4/6 inhibitors in combination with gemcitabine and taxanes (docetaxel) that are employed in the treatment of pancreatic cancer (6). Mechanistically, the anti-neoplastic activities of gemcitabine and docetaxel rely on independent mechanisms (46, 47). Gemcitabine functions both to limit nucleotide pools and incorporates into DNA to further disrupt DNA synthesis (48). Contrasting findings have emerged relative to the influence of CDK4/6 inhibition on response to gemcitabine. In breast cancer models, combination of CDK4/6 inhibitor with gemcitabine led to an antagonistic mode of interaction; however, in PDAC models there have been variant responses that appear to be modified by the level of RB protein (23). In our models which are all RB positive, gemcitabine treatment appears to be dominant where veritably all cells were arrested in S-phase even in the presence of palbociclib. Gemcitabine-mediated S-phase arrest

is characterized by limited cyclin D1 expression and hyperphosphorylated RB, which were not modulated by palbociclib. Not surprisingly, the cytotoxic effect of gemcitabine was also not altered in the PDAC models. However, in long-term outgrowth assays that mimics the use of CDK4/6 inhibitors as maintenance therapy following chemotherapy, we observed the cytostatic response of CDK4/6 inhibitors to be more prominent thereby limiting the colony formation. These data suggest that following the cessation of chemotherapeutic agents that target DNA replication, the cells re-enter cell-cycle with baseline DNA damage that primes them to be more sensitive to the cytostatic effect of CDK4/6 inhibition. Previous studies have shown antagonistic mode of interaction between CDK4/6 inhibitors and DNA damaging drugs including gemcitabine in breast cancer models, which contradicts our observation in PDAC models (22, 23). However, in this study we have clearly shown that the effect of CDK4/6 inhibition in breast cancer derived MCF7 cells is more robust and significantly blocks the cells to undergo G1-S phase transition. Such phenomenon could protect the cells from the chemotherapy-induced toxicity that requires active cell-cycle progression. In support of this notion, in our current study we induced a complete G1 arrest in the PDAC cells by depleting cyclin E1 expression that enhances the cytostatic effect of palbociclib thereby preventing the S-phase entry. Under this condition, the PDAC cells were significantly protected from the cellular effects of gemcitabine. However, the likelihood to achieve such robust cell-cycle arrest by CDK4/6 inhibitor in a clinical setting is improbable in PDAC or in other RAS-driven cancers. Therefore, concerns related to antagonism may be overstated in the context of RB-proficient tumor types (24, 25).

In contrast to gemcitabine, taxanes impinge on spindle dynamics that lead to mitotic catastrophe and other forms of chromosome damage due to inappropriate progression through mitosis (37). In pancreatic cancer there is clear evidence that taxanes induce transient mitotic arrest that allowed them to prematurely exit mitosis and undergo re-replication. Interestingly, while CDK4/6 inhibition has little effect on progression into mitosis in PDAC models, it potently prevents taxane-mediated DNA re-replication in an RB dependent manner by cooperatively limiting CDK2-kinase activity through the downregulation of cyclins that drive resistance. The enhanced cytostatic effect of CDK4/6 inhibition in combination with taxane further limited the outgrowth of PDAC cells. Similar to gemcitabine, by inducing a stronger cell-cycle arrest, PDAC cells could be protected from the cellular effects of docetaxel. Depletion of endogenous CDK2 enhances the cytostatic effect of palbociclib and blocks the progression of cells through G2-phase. Under this condition, the PDAC cells could be protected from the cellular and cytotoxic effects of docetaxel.

Since the combination of gemcitabine and taxane is commonly used in the treatment of metastatic PDAC, we also modeled this therapy in organoid cell cultures and *in vivo* using PDX models (6). Based on the organoid formation it is very clear that the combination of gemcitabine and taxane is clearly superior to the individual chemotherapy agents. However, the inclusion of CDK4/6 inhibitor to chemotherapy drugs clearly improved the cytotoxic effects of these agents. Consistent with this observation, PDX models also showed a more durable disease control in the presence of CDK4/6 inhibitors in combination with chemotherapy drugs as compared to chemotherapy alone. Additionally, the chemotherapy treatment resulted in disease progression after the cessation of treatment; whereas inclusion

of CDK4/6 inhibitor drove stable disease control. These findings agree with other studies that there is a potential to use CDK4/6 inhibitors in concert with chemotherapy (26, 27).

In conclusion, we provide a preclinical proof of concept that the cellular response of CDK4/6 inhibitors could be enhanced in combination with chemotherapy agents by exploiting their distinct mechanisms of actions (particularly taxanes). Moreover, the findings from the present study would support the use of CDK4/6 inhibition in a "maintenance setting" where they could limit selection during chemotherapy response and be continued when chemotherapy has to cease due to cumulative toxicity. Notably the CDK4/6 inhibitor could preclude the growth of residual cells that survive chemotherapy cytotoxicity, while presumably the chemotherapy will kill those cells that evade the CDK4/6 inhibitor.

Methods

Cell lines and growth media

Primary PDAC cells were cultured in Keratinocyte SFM medium, supplemented with EGF (0.2 ng/mL), bovine pituitary extract (30 μg/mL) (Life Technologies, Carlsbad, CA) and 2% fetal bovine serum (FBS) on a collagen-coated (Millipore, Burlington, MA) tissue culture dishes. Select PDAC models were transduced to express H2B-GFP as an independent measure for proliferation. Breast cancer derived, MCF7 cells were maintained in DMEM medium containing 10% FBS. All the cells lines were grown at 37°C and 5% CO_2 and were confirmed to be mycoplasma free.

siRNA transfections

PDAC cells were reverse transfected using Dharmacon Human siGENOME siRNA: Cyclin E1 (M-003213–02-0005) and non-targeting siRNA (D-001810–10-05) and CDK2 siRNA (ID# 103569) was purchased from Thermo Fisher. Transfection was carried out using Lipofectamine RNAiMax Transfection Reagent (Invitrogen, 13778150) by following the manufacturer's protocol. Following 24 h transfection, cells were exposed to different drugs up to 48 H. Parallel experiments were performed using immunoblot analysis to confirm gene silencing.

In vitro CDK2 kinase assay

The CDK2 kinase activity in the PDAC cells were determined by measuring the phosphorylation of an exogenous RB C-terminal substrate, which was bacterially purified (41). See Supplementary information for details.

Flow Cytometry Cell-cycle analysis

PDAC cells were pulsed with BrdU for 4 h before harvesting. The cells were then processed for cell-cycle analysis using a BD LSRFORTESSA flow cytometer. See Supplementary information for details.

Mice and xenografts

NSG mice were maintained at University of Arizona animal care facility. All animal care, drug treatments and sacrifice were approved by the University of Arizona Institutional

Animal Care and Use Committee (IACUC) in accordance with the NIH guide for the care and use of laboratory animals. See Supplementary information for details.

Gene expression analysis

RNA was isolated form the PDAC cell line, MCF7 cells and the snap-frozen PDX tumor tissues using RNeasy Plus kit (Quiagen). Resultant RNA was used for 50 bp paired-end RNA sequencing as described before (19, 28). The differentially expressed genes were generated based on the average log fold change of the palbociclib treated groups in the PDAC models relative to the control and the p-value was calculated using Student's one sided lower tail t test. The genes with log fold change lesser than −0.5 and with the false discovery rate greater than 0.05 were considered as downregulated genes and were used to generate the volcano plot. The significantly downregulated genes were then used for Gene Enrichment analysis using ENRICHR to identify the most common gene ontology terms that were ranked based on the p-value. All log-fold change and statistical information is provided in the supplemental data tables S1 and S2.

Data deposition

RNA sequencing data are deposited in GEO: GSE113922.

Supplementary Material

Refer to Web version on PubMed Central for supplementary material.

Acknowledgements

The author thanks all members of the laboratory group and colleagues in the discussion and preparation of the manuscript. The research was supported by a grant to AKW and ESK from National Cancer Institute (NCI).

Competing Interests: Dr. Knudsen and Dr. Witkiewicz have received research funding from Eli Lilly, Novartis and Pfizer over the last 5 years. There is no current research support from these entities and the study was written in the absence of input from any pharmaceutical company.

References

1. Knudsen ES, O'Reilly EM, Brody JR, Witkiewicz AK. Genetic Diversity of Pancreatic Ductal Adenocarcinoma and Opportunities for Precision Medicine. Gastroenterology. 2016;150:48–63. [PubMed: 26385075]
2. Cheema AR, O'Reilly EM. Management of Metastatic Pancreatic Adenocarcinoma. Surg Clin North Am. 2016;96:1391–414. [PubMed: 27865284]
3. Siegel RL, Miller KD, Jemal A. Cancer Statistics, 2017. CA Cancer J Clin. 2017;67:7–30. [PubMed: 28055103]
4. Hidalgo M, Cascinu S, Kleeff J, Labianca R, Lohr JM, Neoptolemos J, et al. Addressing the challenges of pancreatic cancer: future directions for improving outcomes. Pancreatology. 2015;15:8–18. [PubMed: 25547205]
5. O'Hayer KM, Brody JR. Personalized therapy for pancreatic cancer: Do we need better targets, arrows, or both? Discov Med. 2016;21:117–23. [PubMed: 27011047]
6. Von Hoff DD, Ervin T, Arena FP, Chiorean EG, Infante J, Moore M, et al. Increased survival in pancreatic cancer with nab-paclitaxel plus gemcitabine. N Engl J Med. 2013;369:1691–703. [PubMed: 24131140]

7. Moore MJ, Goldstein D, Hamm J, Figer A, Hecht JR, Gallinger S, et al. Erlotinib plus gemcitabine compared with gemcitabine alone in patients with advanced pancreatic cancer: a phase III trial of the National Cancer Institute of Canada Clinical Trials Group. J Clin Oncol. 2007;25:1960–6. [PubMed: 17452677]
8. Bailey P, Chang DK, Nones K, Johns AL, Patch AM, Gingras MC, et al. Genomic analyses identify molecular subtypes of pancreatic cancer. Nature. 2016;531:47–52. [PubMed: 26909576]
9. Jones S, Zhang X, Parsons DW, Lin JC, Leary RJ, Angenendt P, et al. Core signaling pathways in human pancreatic cancers revealed by global genomic analyses. Science. 2008;321(5897):1801–6. [PubMed: 18772397]
10. Cancer Genome Atlas Research Network. Electronic address aadhe, Cancer Genome Atlas Research N. Integrated Genomic Characterization of Pancreatic Ductal Adenocarcinoma. Cancer Cell. 2017;32:185–203 e13. [PubMed: 28810144]
11. Schutte M, Hruban RH, Geradts J, Maynard R, Hilgers W, Rabindran SK, et al. Abrogation of the Rb/p16 tumor-suppressive pathway in virtually all pancreatic carcinomas. Cancer Res. 1997;57:3126–30. [PubMed: 9242437]
12. Cowan RW, Maitra A. Genetic progression of pancreatic cancer. Cancer J. 2014;20:80–4. [PubMed: 24445769]
13. Witkiewicz AK, McMillan EA, Balaji U, Baek G, Lin WC, Mansour J, et al. Whole-exome sequencing of pancreatic cancer defines genetic diversity and therapeutic targets. Nat Commun. 2015;6:6744. [PubMed: 25855536]
14. Duronio RJ, Xiong Y. Signaling pathways that control cell proliferation. Cold Spring Harb Perspect Biol. 2013;5:a008904. [PubMed: 23457258]
15. Albanese C, Johnson J, Watanabe G, Eklund N, Vu D, Arnold A, et al. Transforming p21ras mutants and c-Ets-2 activate the cyclin D1 promoter through distinguishable regions. J Biol Chem. 1995;270:23589–97. [PubMed: 7559524]
16. Waddell N, Pajic M, Patch AM, Chang DK, Kassahn KS, Bailey P, et al. Whole genomes redefine the mutational landscape of pancreatic cancer. Nature. 2015;518:495–501. [PubMed: 25719666]
17. Franco J, Witkiewicz AK, Knudsen ES. CDK4/6 inhibitors have potent activity in combination with pathway selective therapeutic agents in models of pancreatic cancer. Oncotarget. 2014;5:6512–25. [PubMed: 25156567]
18. Witkiewicz AK, Borja NA, Franco J, Brody JR, Yeo CJ, Mansour J, et al. Selective impact of CDK4/6 suppression on patient-derived models of pancreatic cancer. Oncotarget. 2015;6:15788–801. [PubMed: 26158861]
19. Knudsen ES, Kumarasamy V, Ruiz A, Sivinski J, Chung S, Grant A, et al. Cell cycle plasticity driven by MTOR signaling: integral resistance to CDK4/6 inhibition in patient-derived models of pancreatic cancer. Oncogene. 2019 Epub ahead of print 29 January 2019; doi: 10.1038/s41388-018-0650-0
20. Francis AM, Alexander A, Liu Y, Vijayaraghavan S, Low KH, Yang D, et al. CDK4/6 Inhibitors Sensitize Rb-positive Sarcoma Cells to Wee1 Kinase Inhibition through Reversible Cell-Cycle Arrest. Mol Cancer Ther. 2017;16:1751–64. [PubMed: 28619757]
21. Iyengar M, O'Hayer P, Cole A, Sebastian T, Yang K, Coffman L, et al. CDK4/6 inhibition as maintenance and combination therapy for high grade serous ovarian cancer. Oncotarget. 2018;9:15658–72. [PubMed: 29644000]
22. Chou A, Froio D, Nagrial AM, Parkin A, Murphy KJ, Chin VT, et al. Tailored first-line and second-line CDK4-targeting treatment combinations in mouse models of pancreatic cancer. Gut. 2018;67:2142–55. [PubMed: 29080858]
23. Witkiewicz AK, Chung S, Brough R, Vail P, Franco J, Lord CJ, et al. Targeting the Vulnerability of RB Tumor Suppressor Loss in Triple-Negative Breast Cancer. Cell Rep. 2018;22:1185–99. [PubMed: 29386107]
24. McClendon AK, Dean JL, Rivadeneira DB, Yu JE, Reed CA, Gao E, et al. CDK4/6 inhibition antagonizes the cytotoxic response to anthracycline therapy. Cell Cycle. 2012;11:2747–55. [PubMed: 22751436]
25. Dean JL, McClendon AK, Knudsen ES. Modification of the DNA damage response by therapeutic CDK4/6 inhibition. J Biol Chem. 2012;287:29075–87. [PubMed: 22733811]

26. Cao J, Zhu Z, Wang H, Nichols TC, Lui GYL, Deng S, et al. Combining CDK4/6 inhibition with taxanes enhances anti-tumor efficacy by sustained impairment of pRB-E2F pathways in squamous cell lung cancer. Oncogene. 2019 Epub ahead of print 30 January 2019; doi: 10.1038/s41388-019-0708-7.
27. Clark AS, McAndrew NP, Troxel A, Feldman M, Lal P, Rosen M, et al. Combination Paclitaxel and Palbociclib: Results of a Phase I Trial in Advanced Breast Cancer. Clin Cancer Res. 2019 Epub ahead of print 11 January 2019; doi:10.1158/1078-0432.CCR-18-0790
28. Knudsen ES, Balaji U, Mannakee B, Vail P, Eslinger C, Moxom C, et al. Pancreatic cancer cell lines as patient-derived avatars: genetic characterisation and functional utility. Gut. 2018;67:508–20. [PubMed: 28073890]
29. Jansen VM, Bhola NE, Bauer JA, Formisano L, Lee KM, Hutchinson KE, et al. Kinome-Wide RNA Interference Screen Reveals a Role for PDK1 in Acquired Resistance to CDK4/6 Inhibition in ER-Positive Breast Cancer. Cancer Res. 2017;77:2488–99. [PubMed: 28249908]
30. Herrera-Abreu MT, Palafox M, Asghar U, Rivas MA, Cutts RJ, Garcia-Murillas I, et al. Early Adaptation and Acquired Resistance to CDK4/6 Inhibition in Estrogen Receptor-Positive Breast Cancer. Cancer Res. 2016;76:2301–13. [PubMed: 27020857]
31. Ewald B, Sampath D, Plunkett W. H2AX phosphorylation marks gemcitabine-induced stalled replication forks and their collapse upon S-phase checkpoint abrogation. Mol Cancer Ther. 2007;6:1239–48. [PubMed: 17406032]
32. Pontano LL, Diehl JA. DNA damage-dependent cyclin D1 proteolysis: GSK3beta holds the smoking gun. Cell Cycle. 2009;8:824–7. [PubMed: 19221502]
33. Pagano M, Theodoras AM, Tam SW, Draetta GF. Cyclin D1-mediated inhibition of repair and replicative DNA synthesis in human fibroblasts. Genes Dev. 1994;8:1627–39. [PubMed: 7958844]
34. Elmore S. Apoptosis: a review of programmed cell death. Toxicol Pathol. 2007;35(4):495–516. [PubMed: 17562483]
35. Hoskins EE, Gunawardena RW, Habash KB, Wise-Draper TM, Jansen M, Knudsen ES, et al. Coordinate regulation of Fanconi anemia gene expression occurs through the Rb/E2F pathway. Oncogene. 2008;27:4798–808. [PubMed: 18438432]
36. Ren B, Cam H, Takahashi Y, Volkert T, Terragni J, Young RA, et al. E2F integrates cell cycle progression with DNA repair, replication, and G(2)/M checkpoints. Genes Dev. 2002;16:245–56. [PubMed: 11799067]
37. Hernandez-Vargas H, Palacios J, Moreno-Bueno G. Molecular profiling of docetaxel cytotoxicity in breast cancer cells: uncoupling of aberrant mitosis and apoptosis. Oncogene. 2007;26:2902–13. [PubMed: 17099726]
38. Shen H, Maki CG. Persistent p21 expression after Nutlin-3a removal is associated with senescence-like arrest in 4N cells. J Biol Chem. 2010;285:23105–14. [PubMed: 20489208]
39. Shangguan WJ, Li H, Zhang YH. Induction of G2/M phase cell cycle arrest and apoptosis by ginsenoside Rf in human osteosarcoma MG63 cells through the mitochondrial pathway. Oncol Rep. 2014;31:305–13. [PubMed: 24173574]
40. Burkhart DL, Sage J. Cellular mechanisms of tumour suppression by the retinoblastoma gene. Nat Rev Cancer. 2008;8:671–82. [PubMed: 18650841]
41. Knudsen ES, Wang JY. Differential regulation of retinoblastoma protein function by specific Cdk phosphorylation sites. J Biol Chem. 1996;271:8313–20. [PubMed: 8626527]
42. Haines E, Chen T, Kommajosyula N, Chen Z, Herter-Sprie GS, Cornell L, et al. Palbociclib resistance confers dependence on an FGFR-MAP kinase-mTOR-driven pathway in KRAS-mutant non-small cell lung cancer. Oncotarget. 2018;9:31572–89. [PubMed: 30167080]
43. Taylor-Harding B, Aspuria PJ, Agadjanian H, Cheon DJ, Mizuno T, Greenberg D, et al. Cyclin E1 and RTK/RAS signaling drive CDK inhibitor resistance via activation of E2F and ETS. Oncotarget. 2015;6:696–714. [PubMed: 25557169]
44. Johnson SM, Torrice CD, Bell JF, Monahan KB, Jiang Q, Wang Y, et al. Mitigation of hematologic radiation toxicity in mice through pharmacological quiescence induced by CDK4/6 inhibition. J Clin Invest. 2010;120:2528–36. [PubMed: 20577054]

45. He S, Roberts PJ, Sorrentino JA, Bisi JE, Storrie-White H, Tiessen RG, et al. Transient CDK4/6 inhibition protects hematopoietic stem cells from chemotherapy-induced exhaustion. Sci Transl Med. 2017;9(387).

46. Pienta KJ. Preclinical mechanisms of action of docetaxel and docetaxel combinations in prostate cancer. Semin Oncol. 2001;28:3–7.

47. Cappella P, Tomasoni D, Faretta M, Lupi M, Montalenti F, Viale F, et al. Cell cycle effects of gemcitabine. Int J Cancer. 2001;93:401–8. [PubMed: 11433406]

48. Heinemann V, Schulz L, Issels RD, Plunkett W. Gemcitabine: a modulator of intracellular nucleotide and deoxynucleotide metabolism. Semin Oncol. 1995;22:11–8.

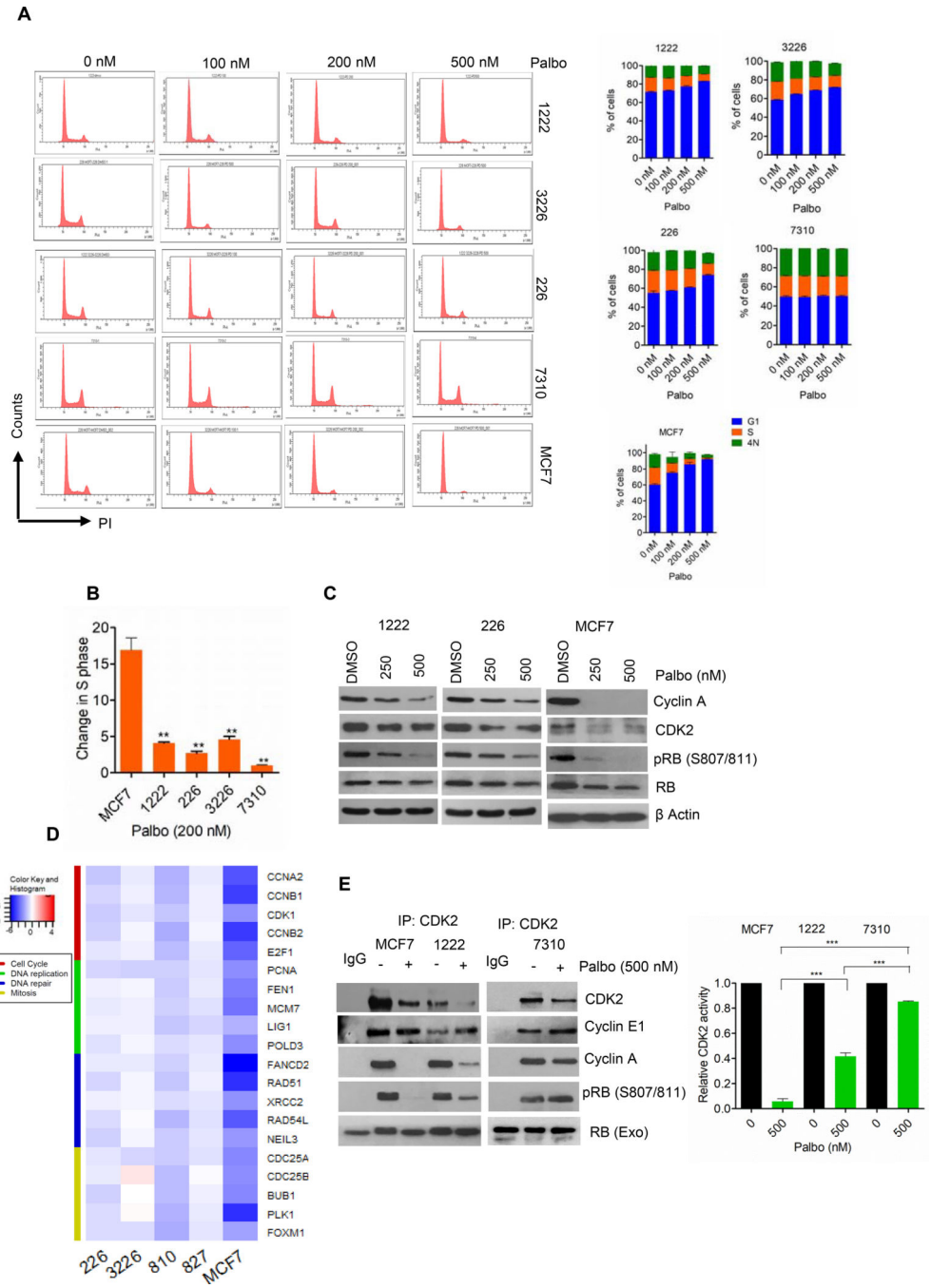

Figure 1: Cellular response of PDAC models and ER$^+$ breast cancer derived MCF7 cell line to palbociclib:

(A) Representative flow cytometric analysis of the indicated PDAC cell lines and MCF7 cells, treated with increasing concentrations of palbociclib up to 48 h. Population of cells at each phase of cell-cycle were quantified. (B) Change in S-phase population between DMSO and palbociclib (200 nM) was determined and shown in the graph. Mean and SD are shown (**p<0.01 as determined by t-test) (C) Immunoblot analysis of the indicated proteins from 1222, 226 and MCF7 treated with different concentrations of palbociclib up to 48 h. (D) Heatmap shows the relative transcriptional repression achieved in the presence of palbociclib

(250 nM) in the indicated cell lines. (E) *In vitro* CDK2 kinase assays were performed using the lysates from MCF7, 1222 and 7310 cell lines that were treated with palbociclib (500 nM). Kinase activity was evaluated based on the site-specific phosphorylation of an RB substrate (S807/811) and the band intensities were quantified. Representative blots, mean and SD are shown (***$p<0.001$ as determined by t-test).

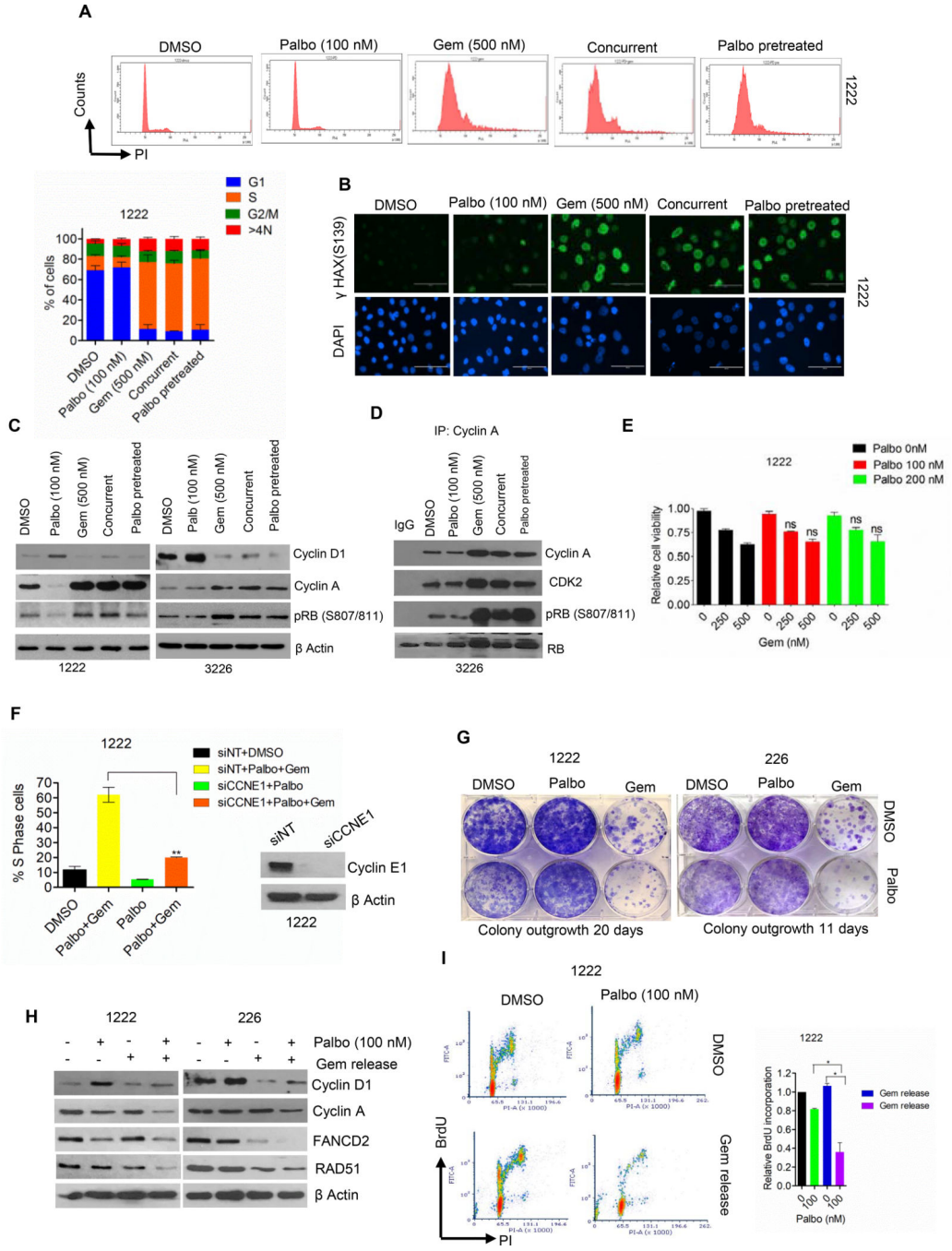

Figure 2: Impact of CDK4/6 inhibition on the cellular effects of gemcitabine.

(A) Representative flow cytometry analysis in 1222 cells, treated with palbociclib (100 nM) for 48 h, gemcitabine (500 nM) for 48 h, Concurrent treatment of palbociclib (100 nM) and gemcitabine (500 nM) for 48 h and palbociclib (100 nM) pretreated for 24 h followed by gemcitabine (500 nM) treatment for 48 h. Cellular population at different phases of cell-cycle were quantified from 3 independent experiments (B) Immunofluorescence staining of γH2AX on 1222 cells treated with palbociclib (100 nM) and gemcitabine (500 nM) under the same conditions as mentioned in (A). (C) Immunoblot analysis on the indicated proteins

from 1222 and 3226 cells treated with palbociclib and gemcitabine under the same conditions as mentioned in (A). (D) *In vitro* cyclin A associated CDK2 kinase assays were performed using the lysates from 3226 cells that were treated with palbociclib and gemcitabine. Kinase activity was evaluated based on the site-specific phosphorylation of an RB substrate (S807/811). (E) Cell viability assay to evaluate the cytotoxic effect of gemcitabine after 96 h exposure in the absence and presence of different concentrations of palbociclib (100 and 200 nM) in 1222 cells. (F) Column graph representing the population of 1222 cells in S-phase. Cells were transfected with non-target siRNA and treated with DMSO (black) and palbociclib (100 nM) in combination with gemcitabine (500 nM) (yellow). Cyclin E1 was depleted using CCNE1 siRNA and the cells were treated with palbociclib (green) alone and in combination with gemcitabine (Orange). Three independent experiments were done and the mean and SD are shown (**$p<0.01$ as determined by t-test). Western blot analysis of cyclin E1 in 1222 cells to confirm the efficacy of RNAi transfection. (G) Cellular outgrowth assay was performed by treating the PDAC cells with gemcitabine (100 nM) up to 48 h and the cells were allowed to re-grow in the absence and presence of palbociclib and stained with crystal violet after the indicated period of time. (H) Immunoblot analysis on the indicated proteins in 1222 and 226 cells following 48 h exposure to palbociclib (100 nM) after releasing the cells from gemcitabine (100 nM). (I) Representative flow cytometry analysis of 1222 cells that were released from Gemcitabine (100 nM) and exposed to palbociclib (100 nM) up to 48 H. X-axis and Y-axis represent DNA content and BrdU incorporation respectively. Relative BrdU incorporation from 3 independent experiments was shown. The mean and SD were shown (* $p<0.05$ as determined by t-test)

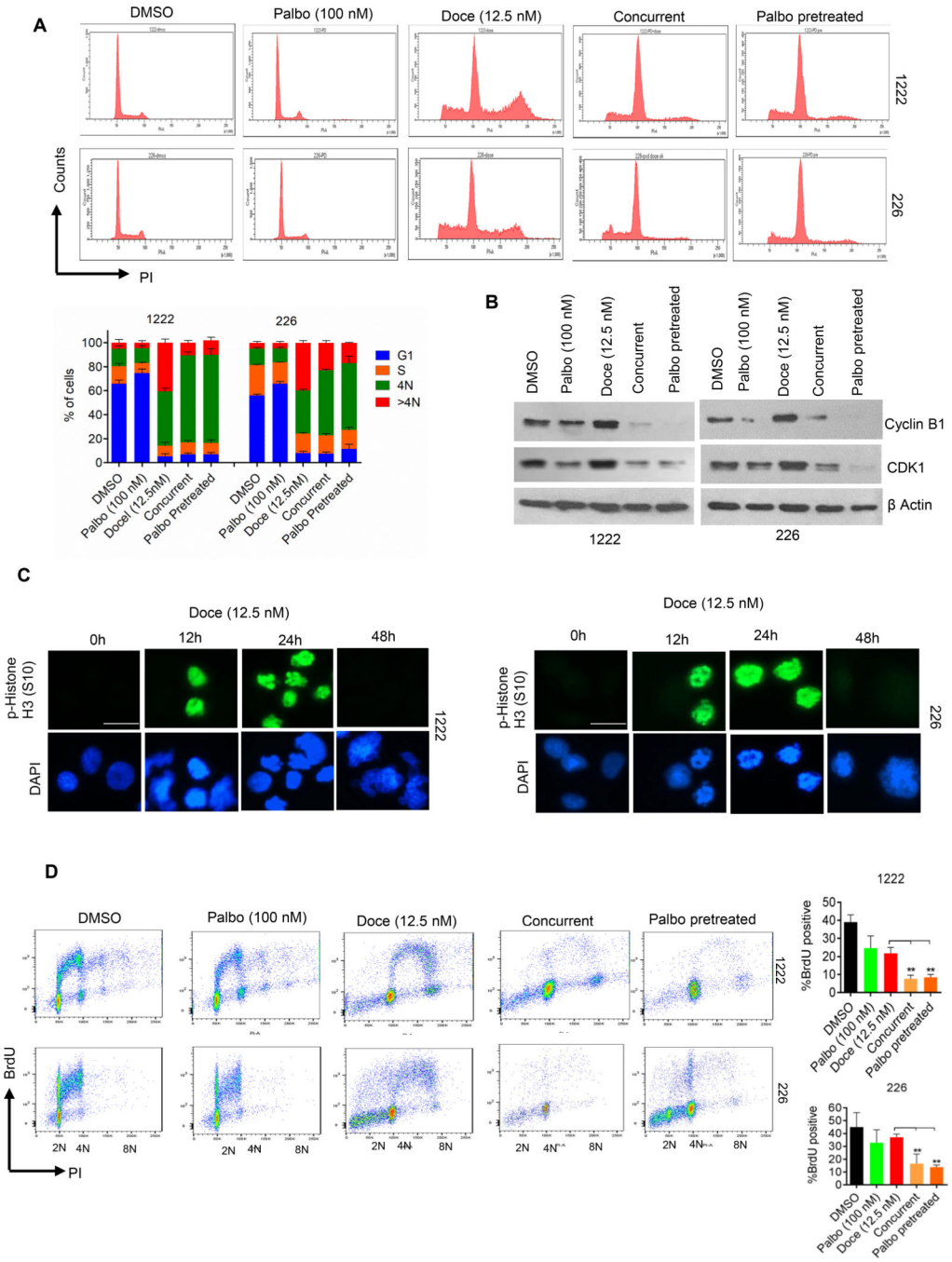

Figure 3: Effect of docetaxel in combination with palbociclib on cell-cycle progression.

(A) Representative flow cytometry analysis of 1222 and 226 cell lines treated with palbociclib (100 nM) for 48 h, docetaxel (Doce) (12.5 nM) for 48 h, Concurrent treatment of palbociclib (100 nM) and docetaxel (12.5 nM) for 48 h and palbociclib (100 nM) pretreatment for 24 h followed by docetaxel (12.5 nM) treatment for 48 h. Quantification of cellular population at different phases of cell-cycle were also shown from 3 independent experiments. (B) Immunoblot analysis in 1222 and 226 cells under the indicated treatment conditions as described in (A), to determine the expression of cyclin B1 and CDK1. β Actin

was included as a loading control. (C) Immunofluorescence staining of p-Histone H3 (S10) on 1222 and 226 cells treated with docetaxel (12.5 nM) at different time points. (D) Representative flow cytometry analysis of 1222 and 226 cell lines at the same treatment conditions as (A). X-axis and Y-axis represent DNA content and BrdU incorporation respectively. Quantification of BrdU positive cells in 1222 and 226 cell lines were shown. The mean and SD are shown (** $p<0.01$ as determined by t-test) from 3 independent experiments.

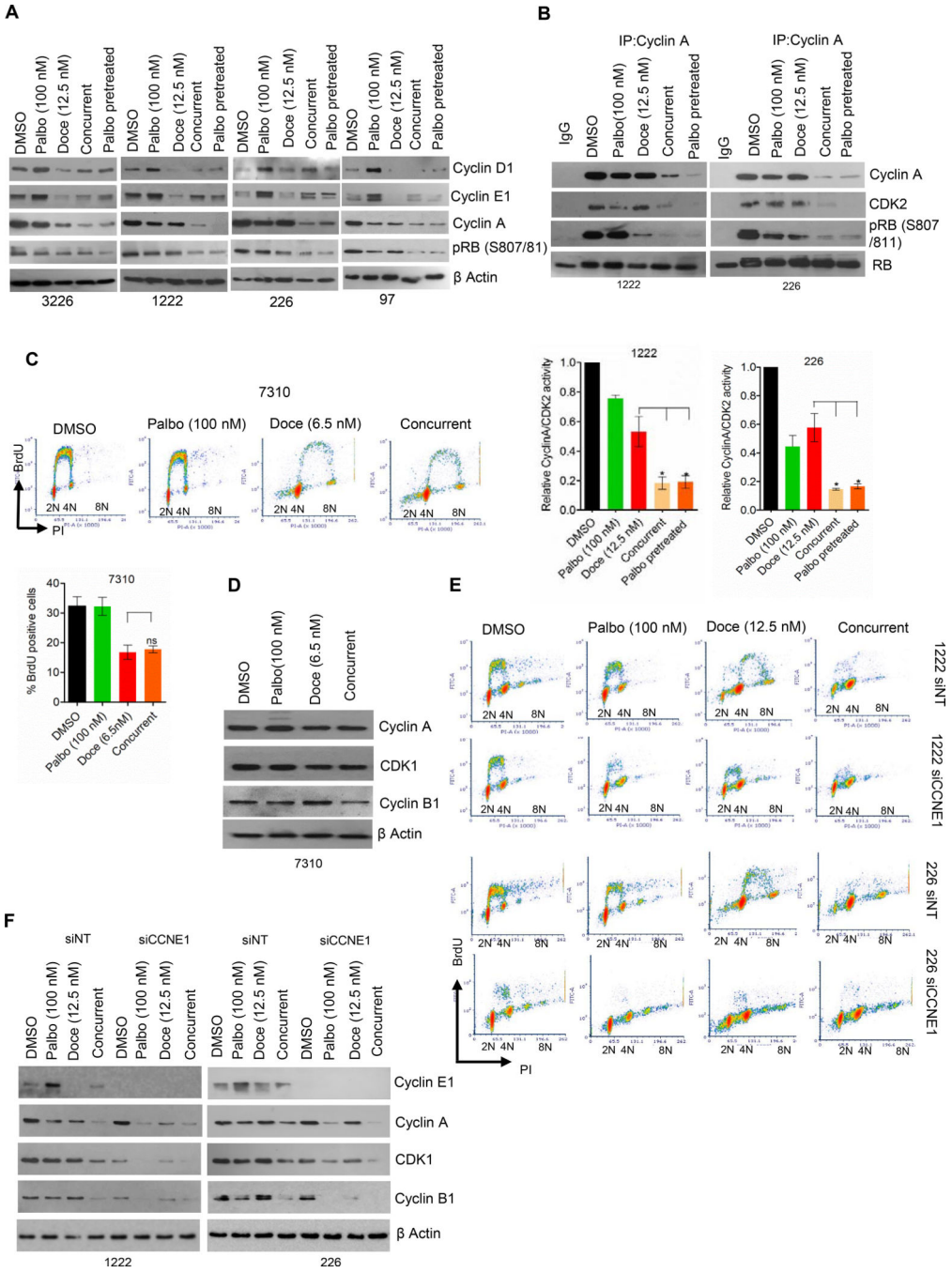

Figure 4: Cooperative cytostatic effect between palbociclib and docetaxel in PDAC models.

(A) Immunoblot analysis on the indicated proteins from 3226, 1222, 226 and 97 PDAC cell lines following 48 h exposure with palbociclib and docetaxel under the indicated conditions. (B) *In vitro* cyclin A associated CDK2 kinase assays in 1222 and 226 cell lines that were treated with palbociclib and docetaxel. Kinase activity was evaluated based on the site-specific phosphorylation of an RB substrate (S807/811) and the band intensities were quantified. Representative blots and mean and SD are shown (*p<0.05 as determined by t-test). (C) Representative flow cytometry analysis of 7310 cells following 48 H exposure with

palbociclib alone and in combination with docetaxel. X-axis and Y-axis represent DNA content and BrdU incorporation respectively. Quantification of BrdU positive cells in 7310 was shown. The mean and SD are shown from 3 independent experiments. (D) Immunoblot analysis in 7310 cells, treated with palbociclib +/− docetaxel to determine the expression of cyclin A and CDK1. (E) Flow cytometry analysis in 1222 and 226 cells that were transfected with non-target siRNA (si-NT) and siCCNE1 followed by exposure to palbociclib +/− docetaxel up to 48 h. X-axis and Y-axis represent DNA content and BrdU incorporation respectively. (F) Immunoblot analysis in 1222 and 226 cells that were transfected with si-NT and siCCNE1 and treated with palbociclib alone and in combination with docetaxel to determine the expression of the indicated proteins.

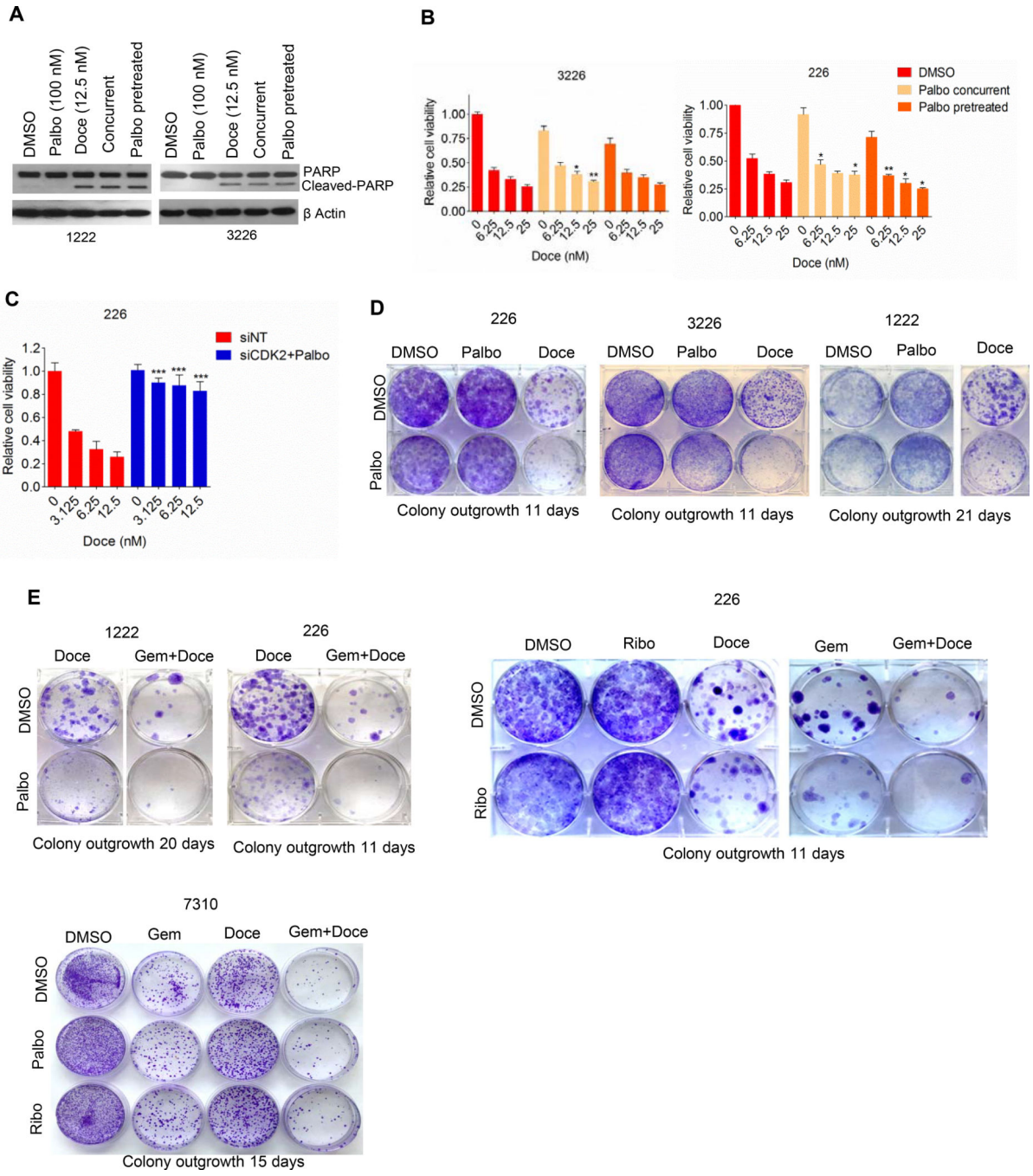

Figure 5: Cooperative cytotoxic effect between palbociclib and chemotherapeutic drugs in PDAC models.

(A) Immunoblot analysis to examine the cleaved PARP levels in 1222 and 3226 cell lines after 96 h exposure with palbociclib +/− docetaxel. (B) Cell viability assay to evaluate the cytotoxic effect of docetaxel after 96 h exposure in the absence and presence of palbociclib (concurrent and 24 h pretreatment) in 3226 and 226 cells. Each drug treatment was performed in triplicates and the experiment was done at two independent times. Mean and SD are shown (*p<0.05, **p<0.01 as determined by t-test). (C) Cell viability assay to evaluate the cytotoxic effect of docetaxel following CDK2 knockdown in combination with

palbociclib following 72 h exposure. Each drug treatment was performed in triplicates and mean and SD are shown (***$p<0.001$ as determined by t-test). (D) Cellular outgrowth assay was performed by treating 1222, 226 and 3226 cells with docetaxel (1.5 nM) up to 48 h and the cells were allowed to re-grow in the absence and presence of palbociclib and stained with crystal violet after the indicated period of time. (E) Cellular outgrowth assay was performed in 1222, 226 and 7310 cells following the treatment with the single and the combinatorial chemotherapeutic drugs (gemcitabine and docetaxel) up to 48 h and the cells were allowed to re-grow in the absence and presence of palbociclib and ribociclib and stained with crystal violet after the indicated period of time.

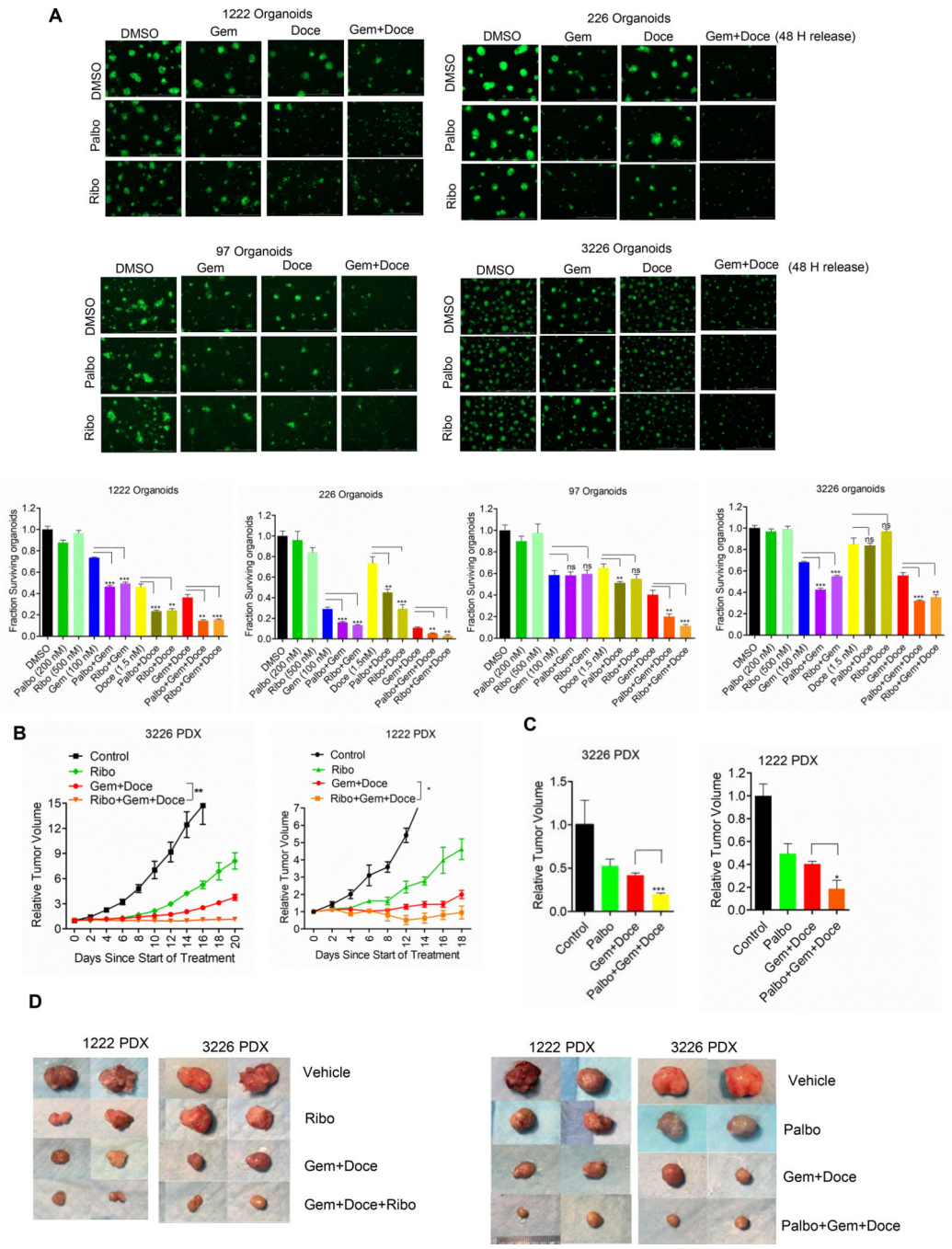

Figure 6: Combination of CDK4/6 inhibitors and chemotherapeutic drugs in PDAC derived organoids and PDX models.

(A) H2B-GFP labelled PDAC cell lines (1222, 226, 3226 and 97) were treated with docetaxel, gemcitabine and gemcitabine in combination with docetaxel (Gem/Doce) up to 48 h and the cells were allowed to form organoids up to 10 days. Organoids from each condition were grown in triplicates and the experiment was performed at two independent times. The viable organoids were quantified using CTG assay and mean and SD are shown (*p<0.05, **p<0.01, ***p<0.001 as determined by t-test). (B) The indicated PDX models were randomized for treatment with vehicle, ribociclib, Gem/Doce, and ribociclib+Gem/

doce when the tumor volume reached 150–200 mm^3. Relative tumor volume was determined every 48 h. Data shows the mean and standard error of mean (*p<0.05, **p<0.001 as determined two-way ANOVA). (C) The indicated PDX models were randomized for treatment with vehicle, palbociclib, Gem/Doce, and palbociclib+Gem/doce up to 21 days when the tumor volume reached 150–200 mm^3. The bar graphs represent the relative tumor volume of the mice under each treatment groups at the end of last treatment. Data shows the mean and standard error of mean (*p<0.05, ***p<0.001 as determined by t-test). The number of mice for 3226 PDX are as follows: Control (n=5), Ribo (n=4), palbo (n=8), Gem +Doce (n=4), Ribo+Gem+Doce (n=5) and Palbo+Gem+Doce (n=5). For 1222 PDX: Control (n=5), Ribo (n=3), Palbo (n=4), Gem+Doce (n=5), Ribo+Gem+Doce (n=3) and Palbo+Gem +Doce (n=3). (D) Representative images of the tumors that were excised from the mice at the end of the treatments.